VOL. 16, NO. 4 J. AIRCRAFT APRIL 1979

79-4049

An Elementary Explanation of the Flutter Mechanism with Active Feedback Controls

Hidetsugu Horikawa* and Earl H. Dowell†
Princeton University, Princeton, N.J.

An elementary explanation of wing flutter suppression problems with active feedback control is made using a standard root locus technique. The object of the study is to obtain insight into the control of converging frequency flutter such as the classical bending-torsion flutter of a wing. The model analyzed is a two-dimensional, typical section airfoil with pure gain feedback of the main wing motion. In this simple system, stability boundary solutions are expressed in a closed form and valuable information is obtained for various kinds of feedback signals. The results for an exploratory example are discussed. The analysis of this example using Nissim's energy method is also attempted.

Nomenclature

b = semichord, ft
C_{L_α} = lift curve slope of the wing
C_{L_δ} = control surface effectiveness
I = moment of inertia about c.m. $= Mr^2$ (lbf·ft·s^2)
K_1 = bending spring constant, lbf·ft^{-1}
K_2 = torsion spring constant, lbf·ft
K_{12}, K_{21} = static structural coupling terms, rad·sec^{-2}
k_A = aerodynamic feedback parameter $(qSbx_pC_{L_\alpha})/I$, s^{-2}
k_y = parameter of bending displacement feedback
$k_{\ddot{y}}$ = parameter of bending acceleration feedback
k_α = parameter of torsion displacement feedback
$k_{\ddot{\alpha}}$ = parameter of torsion acceleration feedback
L = aerodynamic lift force, lbf
M = mass of wing, lbf·ft^{-1}·s^2
M_α = aerodynamic moment, lbf·ft
q = dynamic pressure $\frac{1}{2}\rho V^2$, lbf·ft^{-2}
r = radius of gyration about c.m., ft
S = plan area of typical section, ft^2
s = Laplace transform variable
V = air speed, ft·s^{-1}
x_e = nondimensional location of elastic axis from c.m.
x_p = nondimensional location of aerodynamic center of the wing from c.m.
x_δ = nondimensional location of aerodynamic center of the control surface from c.m.
$x_{P\delta}$ = $(x_P - x_\delta)/x_P$
$x_{\delta e}$ = $(x_\delta - x_e)/x_\delta$
y = nondimensional bending displacement
α = torsion displacement, rad
ω_1 = uncoupled bending frequency, rad·s^{-1}
ω_2 = uncoupled torsion frequency, rad·s^{-1}
ω_δ^2 = $= -(K_1 \cdot bx_\delta \cdot bx_e)/I$
ω_0^2 = $\omega_1^2 (x_P - x_e)/x_P$

I. Introduction

THE concept of a CCV (Control Configured Vehicle) has stimulated the study of active feedback control of wing flutter in recent years.[1] Most of the effort has emphasized the study of an ad hoc problem, whereas only a few works have considered the fundamental aspects of this problem. These ad hoc studies have given rise to various conclusions depending on the system configuration studied. The general trend of the system behavior, however, has been obscured by this type of approach. It is of great importance to obtain physical insight into this complex problem. As a step toward more basic understanding of the effects of various feedback systems, earlier concepts of an elementary explanation of the conventional flutter mechanism[2-4] are extended here to include an active flutter suppression system.[5] The present study introduces the application of a parameter design technique using the root locus method[6] to active flutter control problems of a wing. If a simplified active feedback loop is added to a two-dimensional typical section model, the classical root locus technique for a two-gain problem is applicable. Feedback gains of the system are an aerodynamic parameter k_A, and various active feedback gains k, relating the wing motion to the control surface deflection. For a conventional flutter analysis without any active feedback control, the problem is reduced to a one-gain k_A problem as previously studied in Refs. 2-4.

The proposed feedback loop is a pure gain feedback of wing motion into a trailing-edge flap deflection. Sensed motions of the wing are bending displacement, bending acceleration at the center of mass, torsion displacement, or torsion acceleration. Assuming that the inertial dynamics of the control surface itself is negligible in this case, the number of degrees of freedom of motion of the system can be kept to two, i.e., heaving and rotation of the main wing. Thus, the characteristic polynomial becomes of fourth order and biquadratic. This simplified formulation can show flutter speed trends in concise analytical form.

Another approach applied is Nissium's energy concept.[7,8] As a result, several questions concerning this method arise in the identification of a suitable control system.

II. Typical Section Model with Active Feedback Controls

The simplest bending-torsion flutter model is selected in order to use the standard root locus technique for analyzing system stability and obtain qualitative insight into the flutter suppression system.

The damping terms in the structure and aerodynamics, and hereditary and virtual mass terms in the aerodynamics, are neglected in this converging frequency flutter analysis. This assumption is based on the accumulated experience of theoretical and experimental analyses.[2,3] Omitting the inertia

Received Feb. 1, 1978; revision received Aug. 28, 1978.

Index categories: Guidance and Control; Aeroelasticity and Hydroelasticity; Structural Stability.

*Engineer. Currently with Kawasaki Heavy Industries, Ltd., Kakamigahara, Gifu, Japan.

†Professor, Dept. of Aerospace and Mechanical Sciences. Member AIAA.

and damping effects of the trailing-edge control surface and assuming a pure gain feedback from the sensed motion of the main wing to the control surface, the characteristic polynomial becomes of fourth order and biquadratic. The wing model is shown in Fig. 1. The origin of the coordinate system is located at the center of mass of the model to avoid inertia coupling of the wing and obtain a simple expression in the highest-order coefficient of the characteristic polynomial.

The equations of motion in bending and torsion are derived as follows

$$Mb\ddot{y}+K_1 b(y-x_e\alpha)=L \tag{1a}$$

$$I\ddot{\alpha}+K_2\alpha-K_1 bx_e b(y-x_e\alpha)=M_\alpha \tag{1b}$$

For the aerodynamic operator, static aerodynamic theory is used. Thus the aerodynamic forces and moments on the right hand side of Eqs. (1) are assumed to be proportional to a geometrical angle of attack of the wing or the control surface, i.e.,

$$L=qSC_{L_\alpha}\alpha+qSC_{L_\delta}\delta$$

$$M_\alpha=-qSbx_P C_{L_\alpha}\alpha-qSbx_\delta C_{L_\delta}\delta$$

No formal restriction on the dependence of the aerodynamic coefficients on Mach number is made.

The equations of motion [Eqs. (1)] can be rewritten in the form:

$$\ddot{y}+\omega_1^2 y-\left(K_{12}+\frac{k_A}{x_p}\frac{I}{Mb^2}\right)\alpha=\frac{qSC_{L_\delta}}{Mb}\delta \tag{2a}$$

$$\ddot{\alpha}+(\omega_2^2+k_A)\alpha-K_{21}y=-\frac{qSbx_\delta C_{L_\delta}}{I}\delta \tag{2b}$$

where

$$\omega_1^2\equiv\frac{K_1}{M},\quad \omega_2^2\equiv\frac{b^2x_e^2K_1+K_2}{I},\quad K_{12}\equiv\omega_1^2x_e$$

$$K_{21}\equiv\frac{\omega_1^2b^2x_eM}{I}=K_{12}\frac{b^2}{r^2},\quad k_A\equiv\frac{qSbx_pC_{L_\alpha}}{I}$$

The control surface deflection δ is actuated by four different feedback rules in this study.

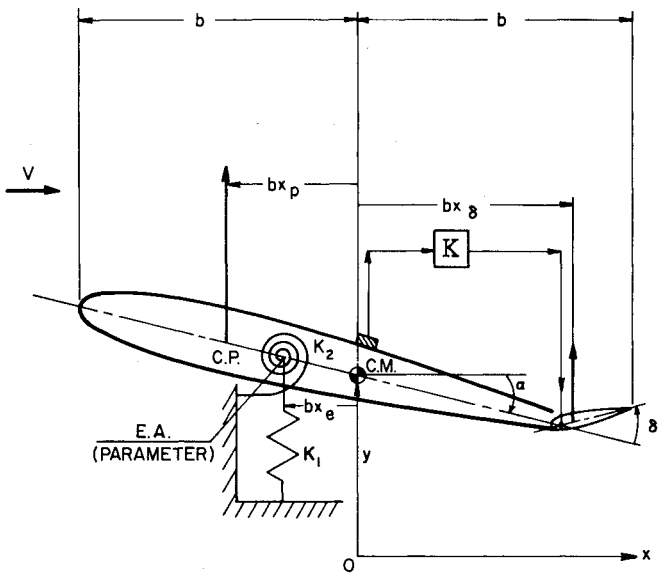

Fig. 1 Typical section airfoil with control surface actuated by active feedback control.

Bending Displacement Feedback

In this case δ is proportional to the bending motion of the wing, $\delta=K_y by$. By using this, the Laplace trasformed characteristic equation of Eqs. (2) reads

$$s^4+(\omega_1^2+\omega_2^2+k_A-k_Ak_y)s^2+\omega_1^2\omega_2^2-K_{12}K_{21}+k_A\omega_0^2$$
$$-k_Ak_y(\omega_2^2+\omega_\delta^2+k_Ax_{P\delta})=0$$

where

$$k_y=\frac{C_{L_\delta}r^2}{C_{L_\alpha}bx_P}K_y,\quad \omega_0^2=\omega_1^2\frac{x_P-x_e}{x_P}$$

$$\omega_\delta^2=-\omega_1^2\frac{b^2x_\delta x_e}{r^2},\quad x_{P\delta}=\frac{x_P-x_\delta}{x_P}$$

In order to study the effect of the aerodynamics and the active feedback control on the system stability by the root locus method, the aerodynamic and feedback control operators must be separated from the structural parameters of the system as follows:

$$s^4+(\omega_1^2+\omega^2{}_2)s^2+(\omega_1^2\omega_2^2-K_{12}K_{21})+k_A(s^2+\omega_0^2)$$
$$-k_Ak_y(s^2\omega_2^2+\omega_\delta^2+k_Ax_{P\delta})=0 \tag{3}$$

Bending Acceleration Feedback

Using the same procedure except $\delta=K_{\ddot{y}}b\ddot{y}$, the following form is obtained for this configuration:

$$s^4+(\omega_1^2+\omega_2^2)s^2+(\omega_1^2\omega_2^2-K_{12}K_{21})+k_A(s^2+\omega_0^2)$$
$$-k_Ak_{\ddot{y}}s^2(s^2+\omega_2^2+\omega_\delta^2+k_Ax_{P\delta})=0 \tag{4}$$

where

$$k_{\ddot{y}}=\frac{C_{L_\delta}r^2}{C_{L_\alpha}bx_P}K_{\ddot{y}}$$

Torsion Displacement Feedback

$\delta=K_\alpha\alpha$

$$s^4+(\omega_1^2+\omega_2^2)s^2+(\omega_1^2\omega_2^2-K_{12}K_{21})+k_A(s^2+\omega_0^2)$$
$$+k_Ak_\alpha(s^2+\omega_1^2x_{\delta e})=0 \tag{5}$$

where

$$k_\alpha=\frac{C_{L_\delta}x_\delta}{C_{L_\alpha}x_P}K_\alpha\qquad x_{\delta_e}=\frac{x_\delta-x_e}{x\delta}$$

Torsion Acceleration Feedback

$\delta=K_{\ddot{\alpha}}\ddot{\alpha}$

$$s^4+(\omega_1^2+\omega_2^2)s^2+(\omega^2{}_1\omega_2^2-K_{12}K_{21})+k_A(s^2+\omega_0^2)$$
$$+k_Ak_{\ddot{\alpha}}s^2(s^2+\omega_1^2x_{\delta e})=0 \tag{6}$$

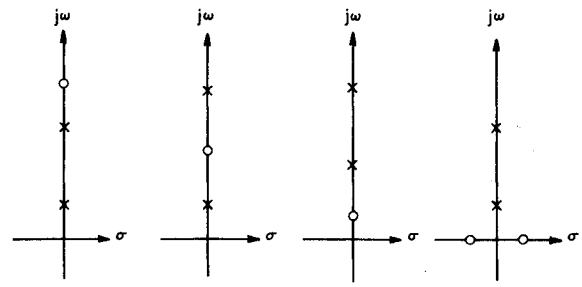

Fig. 2 Basic pole-zero constellation (from Ref. 4).

where

$$k_{\ddot{\alpha}} = \frac{C_{L_\delta} x_\delta}{C_{L_\alpha} x_P} K_{\ddot{\alpha}}$$

Velocity signal feedback of bending and torsion is known to be ineffective in this simplified system and was not attempted.[5]

III. Parametric Stability Analysis

The characteristic polynomial of Eq. (3) can be written in a form amenable to the root locus method:

$$1+G=1+K(N/D)=1-k_y k_A \times \frac{s^2+\omega_2^2+\omega_\delta^2+k_A x_{P\delta}}{s^4+(\omega_1^2+\omega_2^2)s^2+\omega_1^2\omega_2^2-K_{12}K_{21}+k_A(s^2+\omega_0^2)}=0 \quad (7)$$

The denominator of G was discussed in Ref. 4 in some detail. A more precise and exact discussion will be carried out here for clarity. This denominator D is also reduced to the following form

$$1+G_d=1+K_d(N_d/D_d)=1+k_A \times \frac{s^2+\omega_0^2}{s^4+(\omega_1^2+\omega_2^2)s^2+\omega_1^2\omega_2^2-K_{12}K_{21}}=0 \quad (8)$$

The four poles of this transfer function G_d represent physically the undamped structurally coupled frequencies of the bending-torsion model. Due to the symmetry of the pole-zero constellation of the transfer function, one can identify four different pole-zero topologies as indicated in Ref. 4 (see Fig. 2). In general, the aerodynamic parameter k_A can assume both positive and negative values. The resulting eight stability patterns exhaust all possible parameter variations.

If several different control devices are added to those patterns, many more configurations can occur. Since our interest is in the suppression of flutter, the configurations which have the most practical combinations of center of mass, elastic axis, and center of the pressure and which induce flutter phenomena are selected for further study including active feedback control. In this paper the center of pressure and the elastic axis exist in front of the center of mass (x_e and $x_p<0$). The bending mode frequency is lower than the torsion one. The probable root loci of Eq. (8) for this configuration are shown in Fig. 3. These loci indicate the location of the poles of Eq. (7) for a certain fixed aerodynamic gain k_A.

The location of zeros of Eq. (7) is obtained by

$$1+k_A \frac{x_{p\delta}}{s^2+\omega_2^2+\omega_\delta^2}=0 \quad (9)$$

where $x_{P\delta}$, $\omega_\delta^2>0$, $k_A<0$ for the configuration studied. The locus of zeros for k_A is as in Fig. 4.

For a certain fixed aerodynamic parameter k_A, characteristic roots of the system move from poles which are located somewhere on the pole loci in Fig. 3 to zeros located somewhere on the zero loci in Fig. 4, as the active feedback gain k_y varies. The solution sought is the one which stabilizes flutter by the introduction of various types of feedback control configurations.

Because the characteristic polynomials of Eqs. (3-6) are biquadratic, the system is at most marginally stable and can be investigated by using $\bar{s}=s^2$ as in Ref. 2. The imaginary axis in the s plane which gives marginal stability is mapped into the negative real axis in the complex $\bar{s}$ plane. The positive real axis in the $\bar{s}$ plane corresponds to the real axis in the s plane. The stability of the system is evaluated by the departure of the root square locus from the negative real axis in the $\bar{s}$ plane. If the locus departs from this axis into the complex plane, flutter occurs. When the locus penetrates the origin from the negative to positive real axis in the $\bar{s}$ plane, the system undergoes divergence.

Substitution of $\bar{s}=s^2$ into Eq. (3) gives

$$\bar{s}^2+(\omega_1^2+\omega_2^2)\bar{s}+(\omega_1^2\omega_2^2-K_{12}K_{21})+k_A(\bar{s}+\omega_0^2) -k_A k_y(\bar{s}+\omega_2^2+\omega_\delta^2+k_A x_{P\delta})=0 \quad (10)$$

Now a simple technique for evaluating stability of the system is available. The analytical condition for a breakaway (departure) point from the negative real axis gives the flutter boundary. First, for the conventional flutter boundary without any active feedback ($k_y=0$), Eq. (10) is rewritten

$$\frac{1}{k_A}=-\frac{\bar{s}+\omega_0^2}{\bar{s}^2+(\omega_1^2+\omega_2^2)\bar{s}+\omega_1^2\omega_2^2-K_{12}K_{21}} \quad (11)$$

The square of the flutter frequency is given by the negative real root of $\partial(1/k_A)/\partial\bar{s}=0$ (breakaway condition). When these roots are substituted back into Eq. (11), the con-

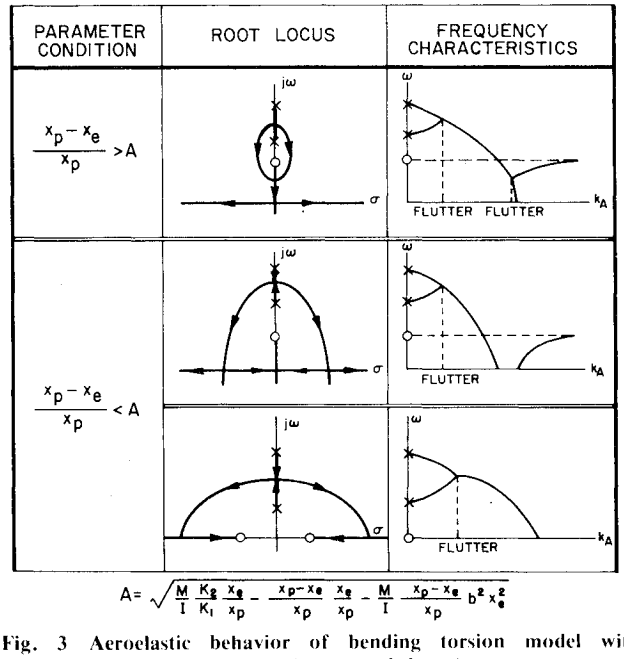

Fig. 3 Aeroelastic behavior of bending torsion model with aerodynamic parameter change (system pole locus).

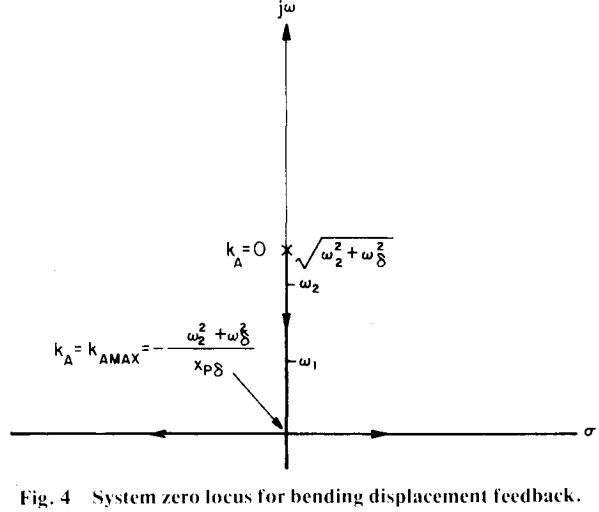

Fig. 4 System zero locus for bending displacement feedback.

ventional flutter boundary is given by

$$k_{AF}=(\omega_0^2-\omega_1^2)+(\omega_0^2-\omega_2^2)$$
$$\pm 2\sqrt{(\omega_0^2-\omega_1^2)(\omega_0^2-\omega_1^2)-K_{12}K_{21}} \tag{12}$$

The positive real root $\bar{s}$ of the breakaway condition is not the stability boundary, but the transition from flutter to divergence.

For the stability boundary of the system with bending displacement feedback loop, Eq. (10) is rewritten

$$\frac{1}{k_y}=k_A\frac{\bar{s}+C}{\bar{s}^2+A\bar{s}+B} \tag{13}$$

where

$$A=\omega_1^2+\omega_2^2+k_A,\quad B=\omega_1^2\omega_2^2-K_{12}K_{21}+k_A\omega_0^2$$
$$C=\omega_2^2+\omega_\delta^2+k_Ax_{P\delta}$$

If one takes $\partial(1/k_y)/\partial\bar{s}=0$, the condition for the breakaway points is $\bar{s}^2+2C\bar{s}+AC-B=0$. Putting the solution of this equation into Eq. (13), the flutter appears as

$$k_{yF}=\{(A-2C)\pm 2\sqrt{C^2+B-AC}\}/k_A \tag{14}$$

Using the same procedure, one can obtain the flutter boundaries for the bending acceleration, torsion displacement, and torsion acceleration feedback systems.

Bending Acceleration Feedback Flutter Boundary

$$k_{\ddot{y}F}=\frac{\bar{s}^2+A\bar{s}+B}{k_A(\bar{s}^2+C\bar{s})} \tag{15}$$

where $\bar{s}$ is the negative root of $(A-C)\bar{s}^2+2B\bar{s}+BC=0$.

Torsion Displacement Feedback Flutter Boundary

$$k_{\alpha F}=\{(2D-A)\pm 2\sqrt{D^2+B-AD}\}/k_A \tag{16}$$

where $D=\omega_1^2x_{\delta e}$.

Torsion Acceleration Feedback Flutter Boundary

$$k_{\ddot{\alpha}F}=-\frac{\bar{s}^2+A\bar{s}+B}{k_A(\bar{s}^2+D\bar{s})} \tag{17}$$

where $\bar{s}$ is the negative root of $(A-D)\bar{s}^2+2B\bar{s}+BD=0$.

A divergence boundary does not appear in this breakaway point condition for the root square locus. This is obtained by the direct inspection of the constant term of the characteristic polynomial. A sign change for this term indicates the divergence boundary. The divergence boundaries for the various feedback configurations are as follows.

Bending Displacement Feedback Divergence Boundary

$$k_{yD}=B/k_AC \tag{18}$$

Bending Acceleration Feedback Divergence Boundary

$$k_{AD}=(\omega_1^2\omega_2^2-K_{12}K_{21})/\omega_0^2 \quad \text{(from origin)}$$
$$k_{AD}=1/k_{\ddot{y}} \quad \text{(from infinity)} \tag{19}$$

Torsion Displacement Feedback Divergence Boundary

$$k_{\alpha D}=-(B/k_AD) \tag{20}$$

Torsion Acceleration Feedback Divergence Boundary

$$k_{AD}=(\omega_1^2\omega_2^2-K_{12}K_{21})/\omega_0^2 \quad \text{(from origin)}$$
$$k_{AD}=-1/k_{\ddot{\alpha}} \quad \text{(from infinity)} \tag{21}$$

IV. Exploratory Example

In order to elaborate upon the preceding results numerically, the following model is used

$$\omega_1=5(\text{rad}\cdot\text{s}^{-1}),\quad \omega_2=10(\text{rad}\cdot\text{s}^{-1}),\quad b=1(\text{ft}),\quad x_m=0,$$
$$x_P=-0.5,\quad x_\delta=0.8,\quad r=1/\sqrt{3}=0.577(\text{ft})$$

The center of mass is located at the midchord. The center of the pressure of the wing is at a quarter chord from the leading edge. The center of pressure of the trailing-edge control surface is assumed to be at 90% chord from the leading edge of the wing. As one of the reviewers has pointed out, the use of the quarter chord for the wing center of pressure and 90% chord for control surface c.p may appear somewhat inconsistent, the former being more representative of subsonic flow and the latter of supersonic flow. This choice of parameter should not be of quantitative importance in the final results, however. These values of wing and control center of pressures are representative of the transonic Mach number regime where the local flow over the airfoil is subsonic near the leading edge and then becomes supersonic near the trailing edge. The location of the elastic axis is a parameter in the range of $-1\le x_e\le 0$ which means the elastic axis moves between the leading edge and the midchord point.

The flutter boundary without any active feedback control is shown in Fig. 5. Flutter instability always occurs for $-1\le x_e\le 0$. If the elastic axis is located behind the center of mass, then only divergence is possible.

The results for the stability boundaries with various active feedback loops are shown in Figs. 6-9. Figure 6 shows the results for the bending displacement feedback system. There are generally four unstable regions, i.e., two for flutter, two for divergence. At $x_e=-1.0$, where the elastic axis is at the leading edge, there is a narrow stable region between two flutter boundaries which makes it difficult to penetrate into

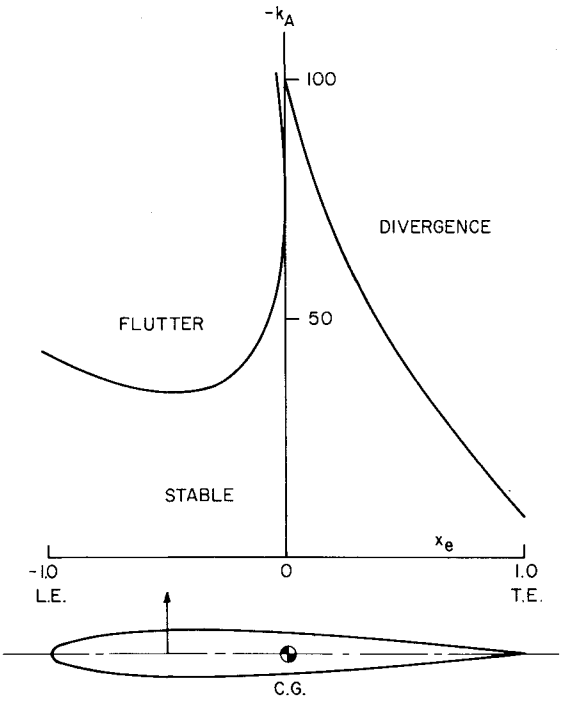

Fig. 5 Critical gain vs location of elastic axis.

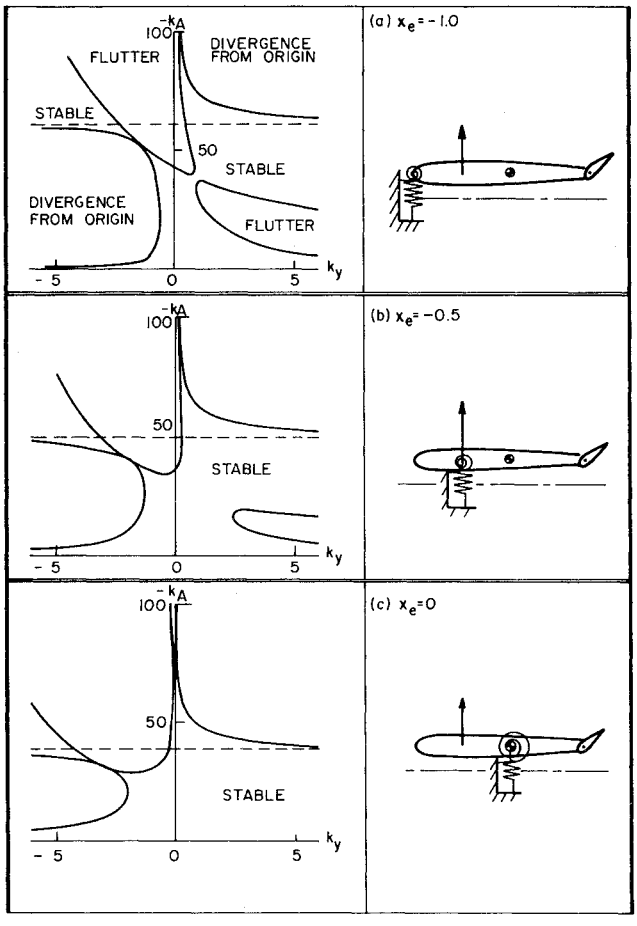

Fig. 6 Stability boundaries of bending displacement feedback system.

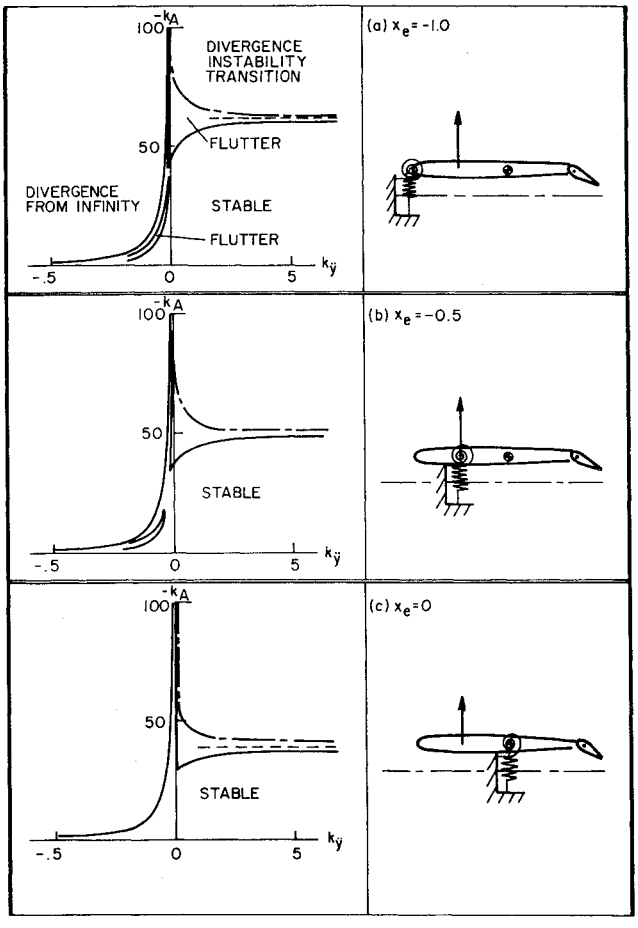

Fig. 7 Stability boundaries of bending acceleration feedback system.

the higher stable region. As the elastic axis goes back toward the center of mass, the narrow stable throat is widened. But, in these cases, the divergence boundaries come down further (Figs. 6b and 6c). As a result, not much improvement can be expected using bending displacement feedback.

Figure 7 is the result for the bending acceleration feedback control. The most interesting feature of this configuration is that the flutter boundary without any feedback control is raised as $k_{\dot{y}}(>0)$ is increased, but its improvement is restricted to a certain limited amount. This ceiling on the flutter boundary is explained as follows. The two zeros of Eq. (7) move as the aerodynamic parameter increases as in Fig. 4. At a certain aerodynamic parameter, these zeros migrate from the imaginary to the real axis through the origin. In the acceleration feedback system, two more zeros are already on the origin of the s plane. Near this aerodynamic parameter, k_A, four zeros are very close to each other. It requires high feedback gain $k_{\dot{y}}$ to stabilize the system when two zeros are close to the origin on the imaginary axis (Fig. 8a). After they are transposed onto the real axis there is no way of stabilizing the system. For this reason, the aerodynamic parameter which locates two zeros on the origin gives rise to a maximum flutter aerodynamic parameter $k_{A\,\max.}$. This is obtained as

$$k_{A\,\max.} = -(\omega_2^2 + \omega_\delta^2)/x_{P\delta}$$

Another interesting feature in the acceleration feedback system is that divergence emerges from positive infinity on the real axis of s plane due to the loss of the leading inertia term in the characteristic polynomial ($k_{\dot{y}} < 0$ in Fig. 7).

Using torsion signal feedback (Figs. 9 and 10) the stability boundaries are simpler compared to the bending signal feedback cases. In the bending signal feedback, there are generally two flutter regions. Since the radicand of Eq. (14) is quadratic in k_A, two positive regions of this radicand can exist which give rise to meaningful $k_{\dot{y}}$. For torsion feedback, on the other hand, there exists only one flutter boundary. In this case, the radicand of Eq. (16) is linear in k_A, and there is only one positive region of this radicand. This is a consequence of the absence of aerodynamic parameter k_A in D of Eq. (16). The two zeros in the torsion feedback do not move at all when k_A varies.

The aerodynamic coupling term from the motion of the main wing is induced only by its torsion motion in this model. The active feedback of torsion motion will reduce the unstable effect of these aerodynamics. On the contrary, pure bending motion of the wing without an active feedback system does not induce any aerodynamic force on this model. Bending signal feedback to the trailing-edge control surface, however, induces torsion motion to the main wing because of the arm length between the elastic axis and the center of the pressure of the control surface. In this case, excessive bending feedback gain may more easily lead this system into instability.

V. Application of Aerodynamic Energy Method

In this section Nissim's energy concept[7,8] is applied to the two-dimensional, typical section model. During flutter, energy must be transferred from the fluid surroundings into the structural system. This statement may be put in another way; namely, a necessary and sufficient condition for flutter prevention is the circumstance that all conceivable, allowable oscillatory motions will require positive work to be done by the model on the surroundings. Let

$[h] = [by, \alpha]$, row vector of displacements

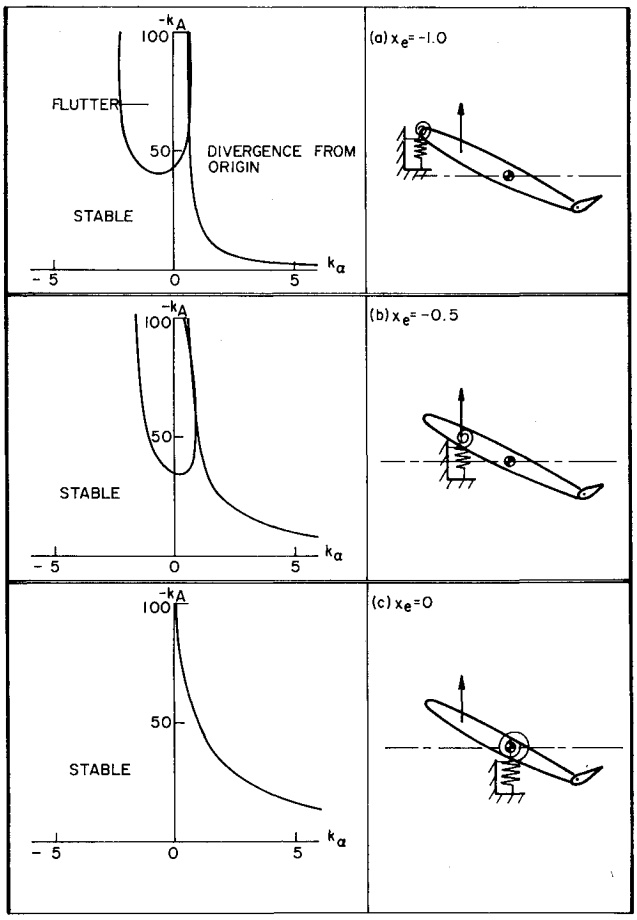

Fig. 8 Ceiling of flutter boundary ($k_{\ddot{y}}$ is the feedback gain).

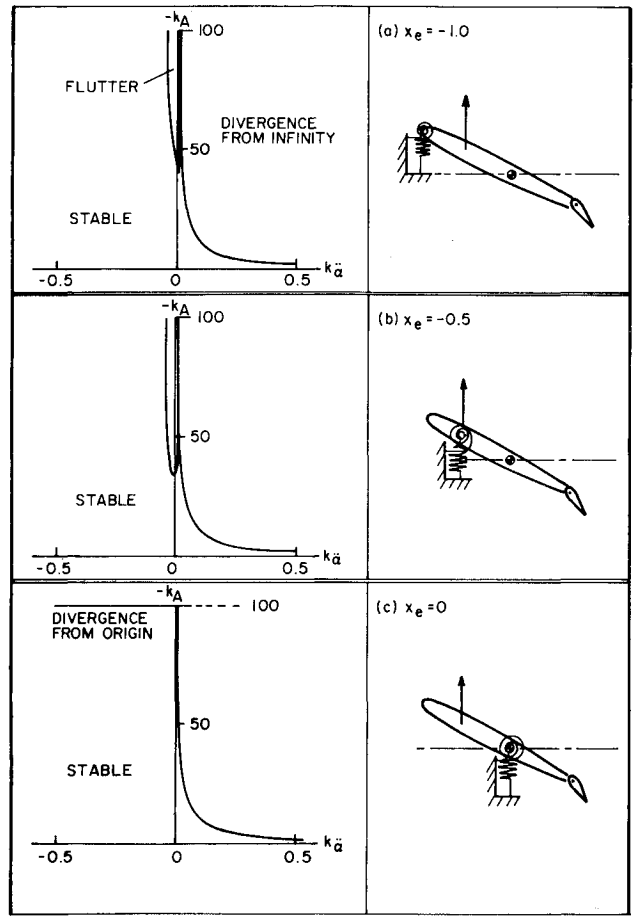

Fig. 9 Stability boundaries of torsion displacement feedback system.

$\{X\} = [V, M]^T$, column vector of forces per unit length which the system exerts on its surroundings; at flutter $\{X\} = 0$. The components of $\{X\}$ are obtained by transferring the right-hand sides in Eq. (1) into the left-hand sides.

$$V = Mb\ddot{y} + K_1 by - K_1 bx_e\alpha - qSC_{L_\alpha}\alpha - qSC_{L_\delta}\delta \tag{22a}$$

$$M = I\ddot{\alpha} + K_2\alpha - K_1 b^2 x_e y + K_1 b^2 x_c^2\alpha + qSbx_P C_{L_\alpha}\alpha + qSbx_\delta C_{L_\delta}\delta \tag{22b}$$

The rate at which the system does work on its surroundings is given by $P = Re[\dot{h}]Re\{X\}$.

In a harmonic motion, only the real parts of $[h]$ and $\{X\}$ need be considered. If this approach is used to analyze the bending displacement feedback system, the components of $\{X\}$ are obtained as follows.

$$\{X\} = (-\omega^2[M] + [S] + qS[A] + qSK_y[C])\{h\}$$

where

$$[M] = \text{mass matrix} = \begin{bmatrix} M & 0 \\ 0 & I \end{bmatrix}$$

$$[S] = \text{stiffness matrix} = \begin{bmatrix} K_1 & -K_1 bx_e \\ -K_1 bx_e & K_2 + K_1 b^2 x_e^2 \end{bmatrix}$$

$$qS[A] = \text{aerodynamic matrix} = qS\begin{bmatrix} 0 & -C_{L_\alpha} \\ 0 & bx_P C_{L_\alpha} \end{bmatrix}$$

$$qSK_y[C] = \text{control matrix} = qSK_y\begin{bmatrix} -C_{L_\delta} & 0 \\ bx_\delta C_{L_\delta} & 0 \end{bmatrix}$$

The real parts of $\{\dot{h}\}$ and $\{X\}$ are given by

$$Re[\dot{h}] = \tfrac{1}{2}i\omega[h_0]e^{i\omega t} - \tfrac{1}{2}i\omega[h_0^*]e^{-i\omega t} \tag{23a}$$

$$Re\{X\} = \tfrac{1}{2}(-\omega^2[M] + [S] + qS[A] + qSK_y[C])\{h_0\}e^{i\omega t} + \tfrac{1}{2}(-\omega^2[M] + [S] + qS[A] + qSK_y[C])\{h_0^*\}e^{-i\omega t} \tag{23b}$$

where * denotes the complex conjugate. The rate of work, i.e., power, is

$$\begin{aligned} \dot{W} = P &= R_e[\dot{h}]R_e\{X\} \\ &= \frac{i\omega}{4}[h_0](-\omega^2[M] + [S] + qS[A] + qSK_y[C])\{h_0\}e^{2i\omega t} \\ &\quad - \frac{i\omega}{4}[h_0^*](-\omega^2[M] + [S] + qS[A] + qSK_y[C])\{h_0\} \\ &\quad + \frac{i\omega}{4}[h_0](-\omega^2[M] + [S] + qS[A] + qSK_y[C])\{h_0^*\} \\ &\quad - \frac{i\omega}{4}[h_0^*](-\omega^2[M] + [S] + qS[A] + qSK_y[C])\{h_0^*\}e^{-2i\omega t} \end{aligned} \tag{24}$$

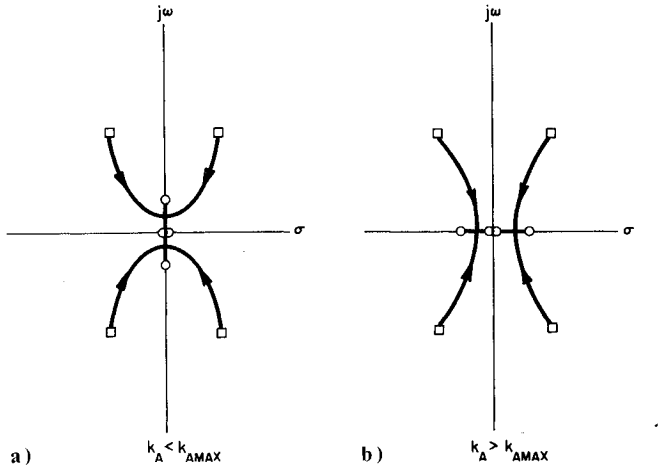

Fig. 10 Stability boundaries of torsion acceleration feedback system.

Hence, the work $\bar{W}$ done per cycle by the structural system on its surroundings can be found by integrating Eq. (24) between $t=0$ to $t=2\pi/\omega$.

Thus,

$$\bar{W}=\frac{i\pi}{2}[h_0](-\omega^2[M]+[S]+qS[A]+qSK_y[C])\{h_0^*\}$$
$$-\frac{i\pi}{2}[h_0^*](-\omega^2[M]+[S]+qS[A]+qSK_y[C])\{h_0\}$$

Since this equation is a scalar equation, the first expression on the right-hand side of this equation can be transposed to obtain

$$\bar{W}=\frac{\pi}{2}[h_0^*][iqS([A]^T-[A])+iqSK_y([C]^T-[C])\{h_0\}$$

$$=\frac{\pi}{2}qSC_{L_\alpha}[h_0^*]$$

$$\times\begin{bmatrix}0 & i\left(1+K_y b x_\delta \frac{C_{L_\delta}}{C_{L_\alpha}}\right)\\ -i\left(1+K_y b x_\delta \frac{C_{L_\delta}}{C_{L_\alpha}}\right) & 0\end{bmatrix}\{h_0\}$$

$$=\frac{\pi}{2}qSC_{L_\alpha}[h_0^*][H]\{h_0\} \tag{25}$$

The conservative force matrices $[M]$ and $[S]$ disappear after integration of $\bar{W}$ through one cycle. The matrix $[H]$ is generally a Hermitian matrix and its eigenvalues are real numbers.

Now the eigenvalues and eigenvectors of the Hermitian matrix $[H]$ are extracted from Eq. (25)

$$[H]\{\eta\}=\nu\{\eta\} \tag{26}$$

The vector $\{h_0\}$ is represented in terms of the eigenvectors of Eq. (26), that is,

$$\{h_0\}=[Q_R+iQ_I]\{\xi_R+i\xi_I\} \tag{27}$$

where $[Q_R]$ and $[Q_I]$ are square matrices whose columns are the real and imaginary parts of the eigenvectors of Eq. (26) and $\{\xi_R+i\xi_I\}$ are the associated generalized coordinates of $\{h\}$.

All the eigenvalue and eigenvector solutions of Eq. (26) can be expressed in the form

$$[Q_R+iQ_I][\nu]=[H][Q_R+iQ_I]$$

Postmultiplying this equation by $\{\xi_R+i\xi_I\}$ and premultiplying it by $[h_0^*]$ or $[\xi_R-i\xi_I][Q_R^T-iQ_I^T]$ yields

$$[\xi_R-i\xi_I][\nu]\{\xi_R+i\xi_I\}=[h_0^*][H]\{h_0\} \tag{28}$$

By using Eq. (28), $\bar{W}$ in Eq. (25) is reduced to the form

$$\bar{W}=\frac{\pi}{2}qSC_{L_\alpha}[\xi_R-i\xi_I][\nu]\{\xi_R+i\xi_I\}$$

$$=\frac{\pi}{2}qSC_{L_\alpha}([\xi_R][\nu]\{\xi_R\}+[\xi_I][\nu]\{\xi_I\}) \tag{29}$$

As shown in Eq. (29) the energy input per cycle into the surroundings has thus been reduced to a quadratic form in terms of the generalized coordinates. The sign of $\bar{W}$, which is the work done by the system on its surroundings per cycle of oscillation, is of importance in the determination of stability. If $\bar{W}$ is positive, then flutter of the system is not possible. If all ν_i's are positive, then the work is positive irrespective of the response of the system, and the system stability will be always guaranteed. This requirement is a sufficient, but not necessary, condition for stability, since the value of $\bar{W}$ can be positive even though some of the ν_i may be negative.

Nissim has proposed that a system which has a larger $\nu_{\min.}$ is a more stable system.[7] This approach has been modified recently by the introduction of the "relaxed energy requirements,"[8] namely, $\nu_{\min.}$ = near maximum value (may be negative) and $\nu_{\max.} \gg |\nu_{\min.}|$. This relaxed requirement is due to the consideration that the variation of a maximum eigenvalue $\nu_{\max.}$ may dominate that of a minimum eigenvalue $\nu_{\min.}$ in some cases.

This energy approach is now applied to Eq. (25). The eigenvalues of $[H]$ are

$$\nu_{1,2}=\pm\left(1+k_y\frac{b^2x_p x_\delta}{r^2}\right)=\pm(1-1.2k_y) \tag{30}$$

It is difficult to evaluate the effect of active feedback gain on this system by using Nissim's method since $\nu_{\max.}=|\nu_{\min.}|$. Moreover, in this example, the real part of the Hermitian matrix is zero. The eigenvalues of this matrix always have a counterpart of opposite sign, i.e., $\pm\nu_1$, $\pm\nu_2$, etc., since the imaginary part of the Hermitian matrix is a skew symmetric matrix. Thus, one can obtain no information about the effectiveness of this control configuration from the eigenvalues in Eq. (30). The importance of the skew symmetric matrix was discussed by Duncan[9] and Crisp.[10] It is this matrix which causes the energy transfer in any converging frequency-type flutter of which bending-torsion flutter is a classical example. In addition, the differences in the stability boundaries among Figs. 6a, 6b and 6c do not show up in Eq. (30). This is clearly due to the lack of inertia and structural stiffness terms in the $[H]$ matrix. The ν's in Eq. (30) do not include any inertia or structural parameters. Hence, the effect of the elastic axis location, which is a crucial structural property of the wing, on system stability is not detected in this energy approach.

The energy method fails to predict the behavior of the flutter suppression system in this particular model. The basic limitation of this approach is in the hypothesis that stability or the degree of stability of the system can be evaluated simply by examining the eigenvalues in the quadratic form of the work $\bar{W}$. In this quadratic form, however, once some of the eigenvalue of $[H]$ are negative, the modal contribution to the work $\bar{W}$ becomes equally important.

It should be said that for single-degree-of-freedom flutter due to negative aerodynamic damping, one would expect

energy methods to be more successful. Real flutter problems are not easily categorized as pure bending-torsion flutter or single-degree-of-freedom flutter. However, the present discussion should serve as a guide as to when energy methods may be useful.

VI. Conclusions

Several interesting conclusions can be drawn.

1) When the flutter is suppressed by decreasing the frequency of a first bending mode branch, bending acceleration feedback can give rise to a ceiling on the flutter boundary even if the feedback gain $k_{\ddot{y}}$ is increased to infinity. More generally, when the system zeros are transposed from the imaginary to the real axis, a ceiling on the flutter boundary is induced by the use of acceleration feedback.

2) A torsion feedback system results in a simpler stability boundary.

3) In the acceleration feedback system, divergence from positive infinity on the real axis of the s plane can occur due to the loss of the leading inertia term in the characteristic polynomial.

4) Zero location of the transfer function is important as indicated in Ref. 11. Not only do zeros show the root locations as gain approaches infinity, they also can be a measure of system behavior.

5) Several questions concerning the utility of Nissim's energy method arise in the identification of a suitable control system for the elementary typical section model studied here.

VII. Applicability and Limitation of the Model

The problem formulation of this simple model imposes no limitations on the flight envelope. Compressibility effects may be accounted for by introducing values of C_{L_α}, C_{L_δ}, and aerodynamic centers appropriate to the flight environment. The discussion presented herein, however, holds only for the simplified flutter model under investigation. When higher-frequency modes participate in the motion, response of the control surface and neglected aerodynamic damping terms will become more important as well as phase shifts in the feedback system. For example, if there is any phase shift in the feedback control laws the system will generally be unstable. To compensate for any anticipated phase shift, a sufficient amount of structural damping will be required to maintain system stability. The neglect of feedback control phase shifts and structural damping is consistent with the neglect of unsteady aerodynamic effects in the present elementary explanation of the bending-torsion flutter mechanism.

Conclusions as to the aeroelastic behavior of an actively controlled practical wing have to be reached with extreme care. Nevertheless the present study should be helpful in interpreting the results from more realistic and complicated analytical models.

References

[1] Ostgaard, M.R. and Swortzel, F.R., "CCVs Active Control Technology Creating New Military Aircraft Design Potential," *Astronautics & Aeronautics,* Vol. 15, Feb. 1977, pp. 42-51.

[2] Pines, S., "An Elementary Explanation of the Flutter Mechanism," *Proceedings of the National Specialists Meeting on Dynamics and Aeroelasticity,* Fort Worth, Texas, Nov. 1958, pp. 52-59.

[3] Zimmermann, N.H., "Elementary Static Aerodynamics Adds Significance and Scope in Flutter Analysis," *AIAA Symposium Proceedings on Structural Dynamics of High-Speed Flight,* 1961, pp. 28-84.

[4] Rheinfurth, M.H. and Swift, F.W., "A New Approach to the Explanation of the Flutter Mechanism," *AIAA Symposium on Structural Dynamics and Aeroelasticity,* Boston, Aug. 30-Sept. 1, 1965, pp. 1-9.

[5] Horikawa, H., "Active Feedback Control of an Elastic Body Subjected to a Nonconservative Force," Ph.D. Thesis, Princeton Univesity; also Dept. of Aerospace and Mechanical Sciences Rept. 1331-T, July 1977.

[6] Dorf, R.C., *Modern Control Systems,* 2nd ed., Addison Wesley, Reading, Mass., 1974, pp. 170-174.

[7] Nissim, E., "Flutter Suppression Using Active Controls Based on the Concept of Aerodynamic Energy," NASA TN D-6199, March 1971.

[8] Nissim, E., "Application of the Aerodynamic Energy Concept to the Selection of Transfer Function for Flutter Suppression and Gust Alleviation Using Active Controls," presented as Paper 77-423 at the AIAA/ASME 18th Structures, Structural Dynamics and Materials Conference, San Diego, Calif., March 21-23 1977.

[9] Duncan, W.J., "Flutter of Systems with Many Freedoms," *Aeronautical Quarterly,* Vol. I, Pt. I, May 1949, pp. 59-76.

[10] Crisp, J.D.C., "The Equation of Energy Balance for Fluttering Systems with Some Applications in the Supersonic Regime," *Journal of Aeronautical Sciences,* Vol. 26, Nov. 1959, pp. 703-711.

[11] "Supersonic Transport Flutter SAS Conceptual Study Results," The Boeing Company, Wichita Division, Rept. D3-7600-9, 1969.